Diode-laser system for high-resolution spectroscopy of the $^2S_{1/2} \rightarrow {}^2F_{7/2}$ octupole transition in ^{171}Yb$^+$

I. Sherstov,[*] M. Okhapkin, B. Lipphardt, Chr. Tamm, and E. Peik

Physikalisch-Technische Bundesanstalt, Bundesallee 100, D-38116 Braunschweig, Germany

A diode-laser system at 467 nm is built in order to drive the $^2S_{1/2} \rightarrow {}^2F_{7/2}$ electric octupole transition at 467 nm in ^{171}Yb$^+$. The frequency of the laser is stabilized to a reference cavity made of ultra low expansion glass and is demonstrated to have a relative instability of better than 2×10^{-15} at 1 s and a stable linear drift rate with variations below 10 mHz/s over several hours. The system is applied for spectroscopy of a single trapped laser-cooled ^{171}Yb$^+$ ion. We obtain excitation spectra of the octupole transition with a resonant excitation probability of about 65% and an essentially Fourier transform-limited resolution of 13 Hz.

The use of laser-cooled and trapped atoms and ions and advances in the techniques of laser frequency stabilization have led to a new generation of highly precise and stable optical atomic clocks [1,2]. The ^{171}Yb$^+$ ion possesses several transitions that are applicable as references for frequency standards, in both the microwave and the optical range [3–5] (see Fig. 1). There are several general features that make this ion attractive: All relevant radiations for cooling and excitation can be generated from diode lasers. A nuclear spin of $\hbar/2$ ensures a simple sublevel structure. Long storage times of Yb$^+$ in ion traps are easily obtained [6]. The $^2S_{1/2}$ ($F = 0$) $\rightarrow {}^2D_{3/2}$ ($F = 2, m_F = 0$) electric quadrupole transition at 436 nm (688 THz) has been recommended as a secondary representation of the SI (International System of units) second. A relative systematic uncertainty of 4.6×10^{-16} has recently been obtained [6]. With a natural linewidth of 3.1 Hz the quantum noise limited instability of a single-ion frequency standard based on this transition is limited at about 2×10^{-15} in 1 s [7]. The electric octupole transition $^2S_{1/2}$ ($F = 0$) $\rightarrow {}^2F_{7/2}$ ($F = 3, m_F = 0$) at 467 nm (642 THz) with a natural linewidth in the nHz range [4] will allow that instability level to be surpassed. In this system the Fourier-limited interrogation linewidth can be adapted to that of the best available laser sources, which are presently at the level somewhat below 1 Hz [8–13].

The frequency of the $^2S_{1/2} \rightarrow {}^2F_{7/2}$ transition is less influenced by external electric and magnetic fields than that of the $^2S_{1/2} \rightarrow {}^2D_{3/2}$ transition. The coefficients of the electric quadrupole shift and of the second-order Zeeman and Stark shifts are significantly lower for the octupole transition [14]. An intuitive explanation for the rather different behavior of the two transitions can be obtained by looking at the dominant electron configurations: while the Yb$^+$ ground state configuration is $5f^{14}6s$, the $^2D_{3/2}$ state has a single electron in the 5d state ($5f^{14}5d$) whereas the $^2F_{7/2}$ level is characterized by a hole in the 5f shell ($5f^{13}6s^2$) which is shielded by the outer 6s electrons. Consequently, the relativistic contributions to both transition frequencies are also quite different, so that the ratio of the transition frequencies is strongly dependent on the value of the fine structure constant α [15]. Measurements of this frequency ratio versus time should allow

a sensitive search for temporal variations of α [14,16]. Such a ratio measurement can be done using a femtosecond laser frequency comb generator, independent of the accuracy and stability limitations of absolute frequency measurements [17]. For the quadrupole transition, a record of precise frequency measurements over a 6-yr span has contributed to obtaining limits on temporal variations of fundamental constants [2,18]. Inclusion of the octupole transition will greatly enhance the sensitivity of these studies.

The realization of a reference laser to drive the $^2S_{1/2} \rightarrow {}^2F_{7/2}$ octupole transition at 467 nm faces two principal challenges: obtaining a narrow linewidth and a sufficient and stable intensity. Since the oscillator strength of the octupole transition is extremely small, an intensity on the order of 1 kW/cm^2 is required to obtain a π-pulse excitation of 0.1 s in duration. This intensity leads to a light shift of the octupole transition frequency of about 100 Hz through coupling to other levels. Both frequency and intensity fluctuations of the laser will lead to line broadening of an excitation spectrum of the octupole transition. In experiments at the National Physical Laboratory (NPL), a frequency-doubled Ti-sapphire laser was used [4,19]. Here we describe a narrow-linewidth diode-laser system capable of resolving the octupole transition in a trapped ^{171}Yb$^+$ ion with a linewidth of 13 Hz and with a resonant excitation probability of 65%.

As shown in Fig. 2 our laser system consists of two 934-nm diode lasers operated in a master-slave configuration. The master laser is an extended-cavity diode laser (ECDL) with an output power of 30 mW. A fraction of this radiation is injected into a slave laser diode with an output power of up to 300 mW for frequency doubling. The slave laser frequency is monitored by means of a frequency comb generator which compares the absolute frequency at 934 nm with references in either the optical or the microwave domain. A fraction of the master laser beam is frequency shifted through an acousto-optical modulator and guided to the reference cavity setup via a polarization maintaining optical fiber for frequency locking to one of the cavity resonances.

The high-finesse reference cavity consists of a 75-mm cylindrical spacer and mirror substrates made of ultra low expansion (ULE) glass. The finesse of the cavity is about 100 000 and its total transmission at resonance is only about 2%. The cavity is placed horizontally in a vacuum chamber where it rests on Viton supports inside a massive
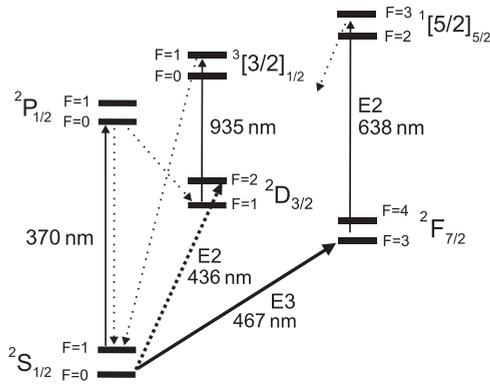
_____
[*]ivan.sherstov@ptb.de

FIG. 1. Simplified level system of ^{171}Yb$^+$ showing the employed laser cooling (370 nm) and repumping excitation (935 nm, 638 nm) and major spontaneous decay paths (dotted lines). Optical clocks can use the dipole-forbidden 436- and 467-nm transitions from the ground state as reference transitions.

FIG. 3. Setup for frequency doubling of 934-nm radiation, showing the beam geometry and polarization orientations in the semimonolithic enhancement cavity. T, transmissivity; HR (AR), high-reflectivity (antireflection) coating.

copper cylinder that provides a homogeneous temperature distribution. The cavity mount has a thermal time constant of more than 24 h. The copper cylinder and the vacuum chamber are temperature stabilized by a two-stage system. The vacuum chamber and the optics used for coupling and stabilization to the ULE cavity are placed on a passive vibration isolation platform with a vertical resonance frequency near 0.5 Hz.

The laser frequency is stabilized to the ULE cavity using the Pound-Drever-Hall scheme [20]. The laser power incident on the cavity is about 100 μW. For phase modulation we use an electro-optical modulator (EOM) operated at 13.5 MHz made of a high-resistivity potassium titanyl phosphate (KTP) crystal with facets cut under Brewster's angle. The use of a KTP crystal results in a particularly low level of residual amplitude modulation. In our case the resulting sensitivity of the locking offset to temperature fluctuations of the KTP crystal is as low as 15 Hz/K so that the temperature of the
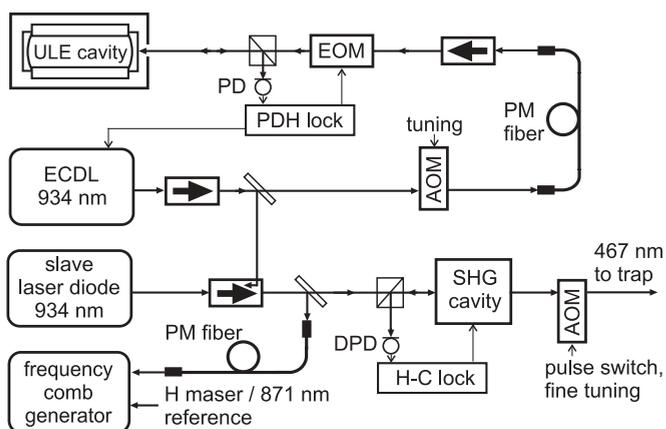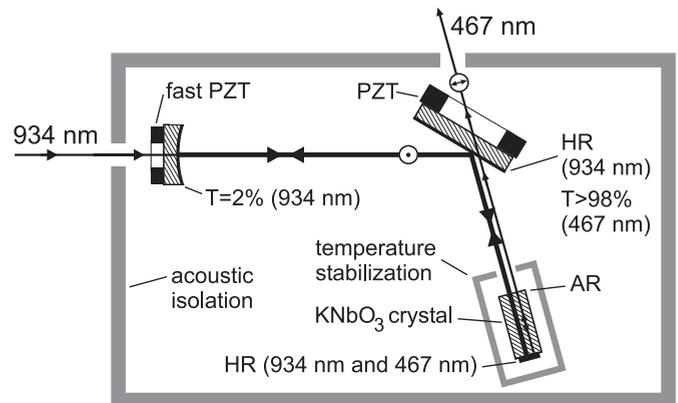

FIG. 2. Schematic setup of the laser system used for excitation of the $^2S_{1/2} \rightarrow \,^2F_{7/2}$ transition of a trapped ^{171}Yb$^+$ ion. ULE, ultra low expansion glass; ECDL, extended-cavity diode laser; AOM, acousto-optic modulator; EOM, electrooptic modulator; (D)PD, (differential) photodetector; PDH (H-C) lock, Pound-Drever-Hall (Hänsch-Couillaud) laser frequency lock electronics; PM fiber, polarization-maintaining single-mode optical fiber; SHG, second-harmonic generation (see also Fig. 3).

phase modulator need not be actively stabilized. The laser frequency is corrected through the laser diode current and by a piezoelectric transducer (PZT) which changes the length of the extended cavity. The frequency control loop has a unity gain frequency of 700 kHz and a $1/f^2$ response at frequencies below 200 kHz.

The main part of the 934-nm radiation is coupled to an enhancement cavity for frequency doubling in a 6-mm-long KNbO$_3$ crystal cut for angle-tuned phase matching at room temperature. The resulting walk-off angle between fundamental and harmonic radiation is $\approx$18 mrad. In order to minimize the walk-off-induced loss in conversion efficiency, a semi-monolithic cavity design was chosen, where one of the end facets of the nonlinear crystal acts as a high-reflectivity (HR) mirror for both the fundamental and the second harmonic radiation [21]. The cavity design is illustrated in Fig. 3. The folded linear cavity is approximately 150 mm long and has an input coupler mirror with a 300-mm radius of curvature. The beam waist in the KNbO$_3$ crystal has the size $w_0 \approx 90$ μm. For efficient outcoupling of the 467-nm radiation, a HR folding mirror for 934 nm is mounted under Brewster's angle for the polarization direction of the second harmonic. Typically more than 90% of 60 mW of incident fundamental laser power is matched into the TEM$_{00}$ mode of the enhancement cavity and 15 mW of 467-nm radiation is produced. The spectral filtering introduced by the enhancement cavity efficiently eliminates spurious broadband components that might be present in the spectrum of the fundamental light. A two-stage Faraday isolator with a specified total isolation of 70 dB suppresses optical feedback to the slave laser diode.

The length of the enhancement cavity is actively stabilized by the Hänsch-Couillaud method [22]. The cavity length is controlled by two PZTs: a fast PZT is attached to the small input coupler mirror and a slower PZT with a wider actuating range is attached to the folding mirror (see Fig. 3). The resulting bandwidth of the HC lock is about 50 kHz and sufficient to efficiently suppress environmental acoustic perturbations. Incompletely suppressed fast-frequency noise of the ECDL leads to relative fluctuations of the SHG power below 10% for Fourier frequencies above 50 kHz.
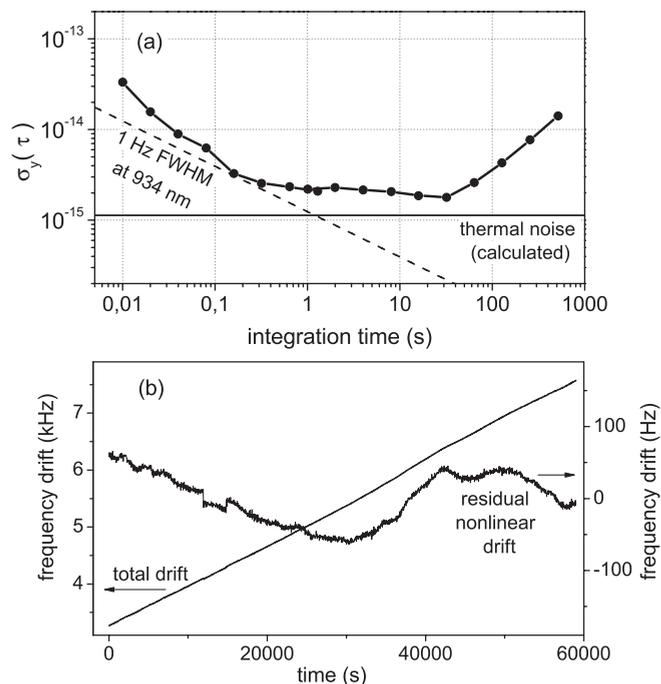
FIG. 4. (a) Combined frequency instability (Allan deviation $\sigma_y(\tau)$ after removal of linear drift) of the employed 934-nm probe laser system and of a similar 871-nm laser system. The dashed line indicates the white frequency noise level that corresponds to a 1-Hz spectral width (FWHM) at 934 nm. The indicated thermal noise level (horizontal line) is the calculated combined thermal noise level (see text). (b) Total drift of the 934-nm laser frequency and nonlinear drift (residuals after subtraction of linear drift of 65 mHz/s) on a magnified scale. The laser frequency was measured relative to a hydrogen maser reference using an averaging time of 100 s.

A small part of the output power of the 934-nm slave diode laser radiation is guided to a fiber-laser-based frequency comb generator that allows us to determine the absolute frequency of the clock laser and its stability [23,24]. In the analysis of the stability the similarly designed probe laser system for the $^2S_{1/2} \rightarrow {}^2D_{3/2}$ transition is used as the reference [6]. The combined instability of both lasers is shown in Fig. 4(a). The observed Allan deviation $\sigma_y(\tau)$ exhibits three distinct domains: For averaging times τ below about 0.1 s, $\sigma_y(\tau)$ decreases roughly like $1/\sqrt{\tau}$. For longer times up to 30 s, $\sigma_y(\tau)$ is essentially constant at about 2×10^{-15}, indicating a $1/f$ dependence of the frequency noise power spectral density. At still longer times the residual drift of both laser frequencies appears. As indicated in Fig. 4(a), the white frequency noise $(1/\sqrt{\tau})$ contribution to the observed instability approximately corresponds to a Lorentzian spectrum with a linewidth of 1 Hz at 934 nm. Consequently we expect that the spectral width of the 467-nm probe radiation is somewhat less than 2 Hz. The observed $1/f$ noise is close to the level calculated according to the thermal noise model of Numata et al. [25] for the two employed reference cavities. The instability characteristic observed here is similar to that of other lasers with linewidths in the Hertz range [8–13]. The limitation imposed by thermal noise reduces the resolution achievable in the recording of narrow spectral lines below 10 Hz in linewidth, especially if averaging over many excitation cycles is required.

The frequency drift of the 934-nm laser was recorded by measuring the absolute frequency relative to a hydrogen maser [see Fig. 4(b)]. The observed drift of the laser is predominantly linear and is around 70 mHz/s. For times of up to 20 h deviations from the average linear drift are typically smaller than 10 mHz/s.

To excite the ^{171}Yb$^+$ $^2S_{1/2} \rightarrow {}^2F_{7/2}$ octupole transition we use the same ion trap and cooling setup as for the 688-THz frequency standard based on the $^2S_{1/2} \rightarrow {}^2D_{3/2}$ quadrupole transition [5,6]. ECDLs are used to produce the cooling radiation at 370-nm wavelength driving the $^2S_{1/2} \rightarrow {}^2P_{1/2}$ transition, and repumping light at 935 and 638 nm is used to deplete the $^2D_{3/2}$ and $^2F_{7/2}$ states, respectively. The probe and and cooling laser radiations are overlapped via a dichroic mirror and are focused to $w_0 \approx 20$ μm at the trap center using an achromatic lens. The overlap between the two foci is adjusted in an equivalent beam path outside the ion trap. Here a pinhole aperture 30 μm in diameter is used to overlap the foci laterally to better than 5 μm and longitudinally to better than one third of the Rayleigh length.

In order to observe the excitation spectrum of the octupole transition, intervals of laser cooling, 370-nm fluorescence detection, and preparation in the $^2S_{1/2}$ ($F = 0$) state are periodically alternated with intervals where the cooling and repumping lasers are blocked and a pulse of 467-nm probe light is applied. In the present experiments, the duration of the laser cooling intervals is 35 ms and probe pulses in the range of 30–120 ms are used. An excitation to the $^2F_{7/2}$ state is registered if no 370-nm fluorescence is observed during the first milliseconds of a cooling cycle but a nonzero fluorescence signal appears during the preceding cooling cycle. After excitation to the $^2F_{7/2}$ state, the ion is returned to the ground state either by stimulated emission during one of the subsequent probe intervals or by repumping light at 638 nm driving the electric quadrupole transition to the $^1D[5/2]_{5/2}$ level (see Fig. 1). Since one of the spontaneous decay paths from the $^1D[5/2]_{5/2}$ level leads back to the $^2F_{7/2}$ state [26], the 638-nm repumping excitation must cover all hyperfine and magnetic sublevels of the $^2F_{7/2}$ state. In the present experiment, this is accomplished by periodically sweeping the frequency of the 638-nm repumping laser over two 200-MHz
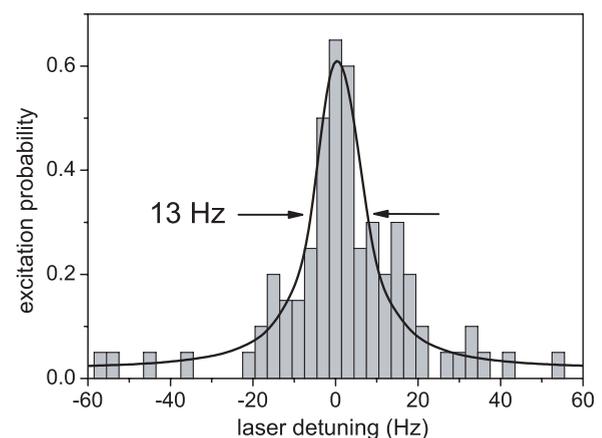

FIG. 5. Observed excitation spectrum of the $^2S_{1/2}$ ($F = 0$) $\rightarrow$ $^2F_{7/2}$ ($F = 3$, $m_F = 0$) transition of a trapped ^{171}Yb$^+$ ion. The superimposed line is a least-squares Lorentzian fit.

intervals separated by the $^2F_{7/2}$ hyperfine splitting frequency of 3.6 GHz. Using a 638-nm laser power of 1 mW focused to $w_0 \approx 50 \ \mu$m, this repumping scheme is sufficient to reduce the average dwell time in the $^2F_{7/2}$ state to the range of 5–10 s. We expect that a more elaborate repumping scheme can reduce the dwell time to the millisecond range.

A high-resolution scan over the ^{171}Yb$^+$ octupole transition is shown in Fig. 5. The scan was taken with 3-Hz steps and 20 interrogation pulses of 90 ms in duration per step. The probe laser power was 1.5 mW. Here, the maximum excitation probability is about 65% and the linewidth (FWHM) of the observed transition fitted by a Lorentzian profile is 13 Hz, demonstrating an essentially Fourier-limited resolution. Spectra were taken for probe laser powers between 0.5 and 7 mW. From these measurements we calculate preliminary values for the light shift coefficient and the absolute transition frequency at zero probe laser power that are in good agreement with the values obtained at NPL [19].

This article has reported results on the precision spectroscopy of the $^2S_{1/2} \rightarrow {}^2F_{7/2}$ electric octupole transition in a single trapped ^{171}Yb$^+$ ion with a resolution in the range of 10 Hz and an excitation probability of more than 60%. These results constitute a significant improvement of the conditions for high-resolution spectroscopy of this line. The achieved high excitation rate of the octupole transition and the predictable frequency drift of our laser system should make it possible to actively stabilize the probe laser frequency to this extremely narrow transition [7]. Controlled periodic variation of the laser power can then be implemented for a continuous monitoring of the light shift, permitting the precise determination of the unperturbed frequency. This opens the perspective for a highly accurate frequency standard based on the octupole transition and for using the optical frequency ratio of quadrupole and octupole transitions in the ^{171}Yb$^+$ ion for a sensitive search for variations of the fine structure constant.

[1] A. D. Ludlow *et al.*, Science **319**, 1805 (2008).

[2] T. Rosenband *et al.*, Science **319**, 1808 (2008).

[3] P. T. H. Fisk, Rep. Prog. Phys. **60**, 761 (1997).

[4] M. Roberts, P. Taylor, G. P. Barwood, P. Gill, H. A. Klein, and W. R. C. Rowley, Phys. Rev. Lett. **78**, 1876 (1997).

[5] T. Schneider, E. Peik, and Chr. Tamm, Phys. Rev. Lett. **94**, 230801 (2005).

[6] Chr. Tamm, S. Weyers, B. Lipphardt, and E. Peik, Phys. Rev. A **80**, 043403 (2009).

[7] E. Peik, T. Schneider, and Chr. Tamm, J. Phys. B **39**, 145 (2006).

[8] B. C. Young, F. C. Cruz, W. M. Itano, and J. C. Bergquist, Phys. Rev. Lett. **82**, 3799 (1999).

[9] M. M. Boyd *et al.*, Science **314**, 1430 (2006).

[10] H. Stoehr, F. Mensing, J. Helmcke, and U. Sterr, Opt. Lett. **31**, 736 (2006).

[11] J. Alnis, A. Matveev, N. Kolachevsky, Th. Udem, and T. W. Hänsch, Phys. Rev. A **77**, 053809 (2008).

[12] J. Millo *et al.*, Phys. Rev. A **79**, 053829 (2009).

[13] P. Dubé, A. A. Madej, J. E. Bernard, L. Marmet, and A. D. Shiner, Appl. Phys. B **95**, 43 (2009).

[14] S. N. Lea, Rep. Prog. Phys. **70**, 1473 (2007).

[15] V. A. Dzuba, V. V. Flambaum, and M. V. Marchenko, Phys. Rev. A **68**, 022506 (2003).

[16] Chr. Tamm, T. Schneider, and E. Peik, Lect. Notes Phys. **648**, 247 (2004).

[17] J. Stenger, H. Schnatz, Chr. Tamm, and H. R. Telle, Phys. Rev. Lett. **88**, 073601 (2002).

[18] E. Peik, B. Lipphardt, H. Schnatz, Chr. Tamm, S. Weyers, and R. Wynands, in *Proceedings of the Eleventh Marcel Grossmann Meeting on General Relativity*, edited by H. Kleinert, R. T. Jantzen and R. Ruffini (World Scientific, Singapore, 2008), p. 941–951.

[19] K. Hosaka, S. A. Webster, A. Stannard, B. R. Walton, H. S. Margolis, and P. Gill, Phys. Rev. A **79**, 033403 (2009).

[20] R. W. P. Drever *et al.*, Appl. Phys. B **31**, 97 (1983).

[21] B. G. Klappauf, Y. Bidel, D. Wilkowski, Th. Chanelière, and R. Kaiser, Appl. Opt. **43**, 2510 (2004).

[22] T. W. Hänsch and B. Couillaud, Opt. Commun. **35**, 441 (1980).

[23] Ph. Kubina *et al.*, Opt. Express **13**, 904 (2005).

[24] T. Nazarova, H. Schnatz, B. Lipphardt, F. Riehle, U. Sterr, and C. Lisdat, in Proceedings of the IEEE Frequency Control Symposium, 2007, joint with the 21st European Frequency and Time Forum, Geneva, 2007, p. 111.

[25] K. Numata, A. Kemery, and J. Camp, Phys. Rev. Lett. **93**, 250602 (2004).

[26] P. Taylor *et al.*, Phys. Rev. A **56**, 2699 (1997).